A vibrational CASSCF study of stretch–bend interactions and their influence on infrared intensities in the water molecule

F. Culot, F. Laruelle*, J. Liévin
Laboratoire de Chimie Physique Moléculaire, CP. 160/09, Université Libre de Bruxelles,
Ave. F.D. Roosevelt, B-1050 Bruxelles, Belgium, Fax: 32-2-6504232, e-mail:jlievin@ulb.ac.be

Summary. An extension of the multiconfigurational SCF approach for the resolution of the vibrational problem is presented; it follows the philosophy of the CASSCF method developed in Quantum Chemistry. The new method allows a more complete treatment of anharmonic mode couplings, converges much faster and gives a clearer physical insight of vibrational interactions. This is exemplified by the calculation of infrared transition moments in the H_2O and D_2O isotopomers of the water molecule. It is shown how this property varies with the quality of the wave function when vibrational resonances occur. A detailed analysis by means of this new VCASSCF method demonstrates the crucial importance of excited bending oscillators in the intensity of some pure stretching transitions.

1 Introduction

A new MCSCF-like method designed for the resolution of the vibrational problem has been presented recently [1]. This method is based on the existence of a generalised Brillouin theorem (GBT) for variationally optimised vibrational wave functions. It has proved to have a more satisfactory behaviour than the classical SCF-CI technique in the cases of strong mode coupling. However, like the traditional MCSCF method widely used to solve the electronic problem, it has several drawbacks:

● The maximum possible size of the configuration expansions is relatively small in MCSCF calculations as compared to MRCI
● Those configurations have to be selected manually, on the basis of previous CI calculations or by physical intuition

---

* Boursier F.R.I.A.

• There are usually some linear dependencies between the variational conditions associated to the CI coefficients and the mode oscillators optimisation (or molecular orbitals, in the electronic context)
• The convergence of the procedure can be slow on some excited states.

In the electronic context, those problems have been solved by the development of the so-called "complete active space" [2] or "fully optimised reaction space" [3] approach, referred to as the CASSCF or FORSSCF methods in Quantum Chemistry. It consists in a particular choice of MC configurations (i.e. the configurations included in the multiconfigurational wave function). Those are obtained by allowing every possible excitation in a limited set of orbitals which forms the so-called "active-space". The set of configurations selected corresponds to a full CI in this subspace. The MC wave function built in that way has a very interesting property; it is invariant to any unitary transformation within the active subset, as any full CI wave function should be. This property limits the number of variational conditions applicable on the molecular orbitals (or mode oscillators) to rotations between active and unoccupied orbitals (or oscillators), the rotations within the active set being redundant with the CI coefficient optimisation.

This paper aims to show how this technique, which proved very successful in Quantum Chemistry, can be applied in the vibrational context. Another aspect of this work is to demonstrate the efficiency of this approach in the interpretation of mode couplings and of their great influence on IR intensities. Those two points will be treated in the case of the water molecule, where a large set of experimental and theoretical data is available.

This paper is separated into two main sections: the first one describes the vibrational CASSCF formalism and its implementation in our VMCSCF algorithm; the second is devoted to the application to H_2O and D_2O.

2 The vibrational CASSCF method (VCASSCF)

The vibrational MCSCF method presented in [1] was based on the generalised Brillouin theorem and used a variation of the super-CI algorithm of Grein and Chang [4]. In order to explain how this procedure can be adapted towards a CASSCF-like optimisation, let us recall the expression of the GBT and the main steps of the MCSCF algorithm which are all preserved, if slightly modified. The reader is sent back to [1] for further details of the procedure.

2.1 The vibrational generalised Brillouin theorem

Let us write the multiconfigurational wave function that we wish to optimise:

$$\Psi_{\mathrm{VMC}} = \sum_i c_i \Psi_i, \tag{1}$$

where Ψ_i represents a vibrational configuration and c_i a configuration interaction coefficient. Ψ_i is a simple product of mode oscillators:

$$\Psi_i = \prod_{\nu=1}^{3N-6} \phi_k^{\gamma}(\xi_\nu), \tag{2}$$

where ξ_v is the vth vibrational coordinate and $\phi_k^v(\xi_v)$ is the corresponding anharmonic oscillator of quantum number k. $\phi_k^v(\xi_v)$ can be developed on a basis set:

$$\phi_k^v(\xi_v) = \sum_{a=0}^{p} d_{ak}\, \Omega_a(\xi_v), \tag{3}$$

where $\Omega_a(\xi_v)$ is a primitive basis function. As discussed for instance in [5], different kinds of primitive one-mode functions can be chosen. In any case, the d_{ak} are the only variational parameters associated with the oscillators basis set.

When the MC wave function (1) is fully optimised with regard to both $\{c_i\}$ and $\{d_{ak}\}$, it complies with the generalised Brillouin theorem. The latter states that all Hamiltonian matrix elements taken between the MC function and its single excitations are zero:

$$\langle \Psi_{\text{VMC}}/H_{\text{vib}}| \Psi_{kl}^v \rangle = 0. \tag{4}$$

Ψ_{kl}^v, which denotes a single excitation, is a multiconfigurational function defined as

$$\Psi_{kl}^v = \sum_i c_i(\Psi_i(v; k \to l) - \Psi_i(v; l \to k)). \tag{5}$$

The notation $\Psi_i(v; k \to l)$ refers to the function obtained by replacing the oscillator of quantum number k by the oscillator of quantum number l, on the mode v in the configuration Ψ_i. The structure and symmetry of the Brillouin single excitations have been detailed elsewhere [1]. This theorem implies that there is no mixing between the MC function and any of its single excitations.

2.2 The VMCSCF optimisation algorithm

Let us first review the successive steps required by the procedure to force a trial function to obey the GBT (i.e. be self-consistent):

1. *Determination of an initial guess for the oscillators basis set* $\{\phi_i\}$. This is usually done by a VSCF calculation on one of the MC configurations or by a previous VMCSCF calculation.
2. *Resolution of the CI problem associated to the configurations of the reference function* Ψ_{VMC} *(MC space).*
3. *Build-up of the single excitations satisfying the Brillouin theorem.* It consists in forming all the single excitations (5). A canonical orthonormalisation is applied in order to eliminate linear dependencies.
4. *Build-up of the Hamiltonian matrix in the basis set formed by the reference and the single excitations (SX space).*
5. *Diagonalisation of the matrix defined at step* 4. The eigenfunction having a dominant coefficient on the MC function is selected; it can be written as

$$\Psi^{\text{ESX}} = a_{00}\, \Psi_{\text{VMC}} + \sum_{v=1}^{3N-6} \sum_{k=0}^{p} \sum_{\substack{l=0 \\ l \neq k}}^{p} a_{kl}\, \Psi_{kl}^v. \tag{6}$$

6. *Transformation of the oscillators basis set.* This transformation is done in order to incorporate the effect of the single excitations in the reference MC function. It is performed according to the following equation, where the oscillators at iteration

$N + 1$ are expressed as a linear combination of the oscillators at iteration N:

$$\Phi_k^\nu(\xi_\nu)^{[N+1]} = a_{kk}^\nu \, \phi_k^\nu(\xi_\nu)^{[N]} + \sum_{l=0, \; l \neq k}^{p} a_{kl}^\nu \, \phi_l^\nu(\xi_\nu)^{[N]}, \tag{7}$$

where the $\{a_{kl}\}$ are fully defined by Eq. (6) plus two relations of norm and orthogonality [1].

7. *Resolution of the CI problem associated to the configurations of* Ψ_{VMC}. This step is equivalent to step 2 except that the configurations are built on the new oscillators basis set defined at step 6.

8. *Back to step 4 and iteration until convergence.*

2.3 The CASSCF philosophy in the vibrational context

As said earlier, the CASSCF approach consists in a particular choice of vibrational configurations; those are taken by performing every possible excitation in a limited oscillators space. This undermines a partition of the mode oscillators basis set in two subspaces: the active set and the virtual set. The active space includes a series of oscillators of quantum number ν starting from 0 up to a user fixed value, which can vary from mode to mode. The virtual set contains the rest of them up to the highest energy oscillators, no "core" oscillators have been defined in our implementation.

It has been shown [2] that, within the active space, the Brillouin theorem is systematically verified, whatever the oscillators basis set. That is,

$$\langle \Psi_{\text{VMC}} / H_{\text{vib}} | \Psi_{k_{\text{act}} l_{\text{act}}}^\nu \rangle = 0, \tag{8}$$

where k_{act} and l_{act} are active oscillators.

The single excitations within the active subspace must no longer be taken into account; they would only create redundancies with the variational conditions associated with the CI coefficients optimisation. The only relevant Brillouin conditions are associated with the single excitations from an occupied (active) to a virtual oscillator as

$$\langle \Psi_{\text{VMC}} | H_{\text{vib}} | \Psi_{k_{\text{act}} l_{\text{virt}}}^\nu \rangle = 0. \tag{9}$$

The single excitation $\Psi_{k_{\text{act}} l_{\text{virt}}}^\nu$ is, furthermore, simpler to create since there is no reverse excitation to consider; we can then equate $\Psi_{k_{\text{act}} l_{\text{virt}}}^\nu$ to the direct excitation $\Psi_i(\nu; k_{\text{act}} \to l_{\text{virt}})$.

The partition of the oscillators basis set in two distinct subspaces is directly reflected in the algorithm: the CI coefficient optimisation is only concerned with the active set and the oscillators optimisation deals only with the virtual set, as summarised in Table 1. This sharp separation between the MC and SX problems prevents any linear dependency that could occur between the variational conditions associated with both sets of coefficients.

2.4 Details of implementation

The algorithm is simplified in two ways: there are fewer single excitations to consider and the remaining ones are simpler. Those modifications are straightforward to implement; one only needs to restrain the single excitations to the virtual space and remove the reverse excitation of them. The manual generation of the MC configurations has also to be replaced by a systematic procedure. The algorithm is

Table 1. Relations between oscillators subspaces and optimisation steps

Oscillators subspace	Optimisation step	Operation performed
Active space	MC problem: optimisation of the MC coefficients	Full CI in the active set
Virtual space	SX problem: Optimisation of the oscillators basis set	Rotation between active and virtual oscillators

made much more efficient and allows to include many more configurations in the calculation. This gives a greater variational flexibility to the wave function and, along with the absence of linear dependencies, allows a much faster convergence.

The possibility of a state average optimisation, which was already present in the original program [1], has been preserved in the CASSCF version. It allows to optimise the oscillators basis set for the average of several states and has the advantage to give a balanced and orthogonal representation of these states, although the averaging imposes a constraint on the wave function, which is no longer fully variational. This option is also very useful when the convergence of the procedure is marred by root flipping problems between closely interacting states.

Our new algorithm has been implemented in the same context as before [1], but the potential energy expansion includes higher-order contributions. We use the Watson [6] Hamiltonian developed in normal coordinates, the inertia matrix has a fixed value, the development of the potential is limited to the sixth-order and the oscillators are expressed as linear combination of harmonic oscillators.

2.5 The convergence of the CASSCF procedure

The convergence of the procedure has been tested on two vibrational states of the ground electronic state of the water molecule, denoted 200 and 002, which correspond to the first overtones of the symmetric and antisymmetric stretch, respectively. Those states interact strongly through a Darling–Dennisson resonance. This particular system has been studied before [1,7] at the VSCF, VSCF-CI and VMCSCF levels. The 002 state was found very difficult to represent properly: the VSCF optimisation on this state led to an inversion of the 200 and 002 states position. This inconsistent behaviour could only be compensated for by the inclusion of a large number of configurations in a subsequent CI calculation. In this case a VSCF optimised basis set is certainly not a good initial guess for a VMCSCF optimisation. Furthermore, with a minimal set of configurations (the lowest-lying 11 configurations of a_1 symmetry plus the 102 one), it has been impossible to optimise separately the 002 by an ordinary VMCSCF procedure; only the average of the two states could be obtained, no matter how carefully the initial guess was prepared. The convergence on these states, especially the 002, starting from the corresponding VSCF oscillators is thus a severe test of the procedure. It has been performed [1], on both interacting states separately at the VCASSCF level, with a basis set of 10 oscillators per mode. We have used for this test an *ab initio* potential energy surface, calculated at a better level of theory (VQZ/MR-CI) than the one adopted in our previous work [1,7] (TZ + 2P/SD-CI). This surface,
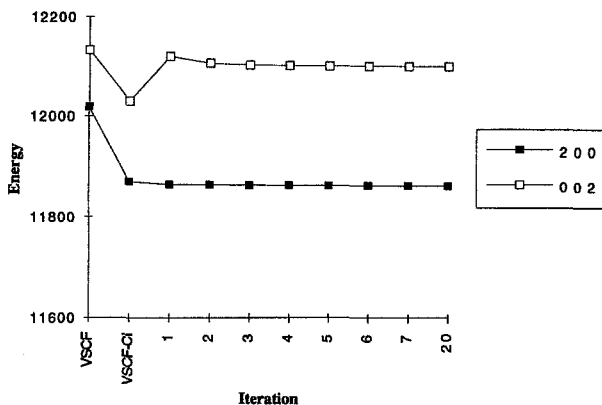
Fig. 1. Convergence of the VCASSCF procedure, applied without state averaging, on the 200 and 002 vibrational states of water

calculated in this work in order to investigate the influence of the quality of the vibrational wave functions on infrared intensities, will be detailed in Sect. 3.1.1.

The active space is defined by the following vibrational quantum numbers:

on the symmetric stretching: $v = 0-3$,
on the antisymmetric stretching: $v = 0-4$,
on the bending: $v = 0-2$.

Taking account of the symmetry, these criteria generate a set of 36 configurations.

The results of this calculation are plotted in Fig. 1 and shows a quasi-perfect convergence after four iterations (0.4 cm^{-1} on average). Let us note that, in the case of the optimisation on the 002 state, the two states are inverted from the VSCF solution to get back to their real position. This explains the surprising shape of the plot which rises sharply and stabilises smoothly afterwards.

3 Application to H$_2$O and D$_2$O

It has been shown in a previous study [7] that the calculation of dipole moment matrix elements is extremely sensitive to the oscillators basis set optimisation, particularly in the cases of vibrational resonances. Off-diagonal (transition) elements are particularly important in vibrational spectroscopy, since they are directly related to infrared transition intensities. The present work aims to study the nature of the vibrational interactions occurring in a particular system and to evaluate their relative importance for the computation of some vibrational transition moments.

The system studied here is the transition from the ground state to the first overtone of the antisymmetric stretch in H$_2$O and D$_2$O (000 → 002), completed by the first corresponding hot band transition (010 → 012) for the H$_2$O isotopomers. The 010 → 012 transition was not computed for D$_2$O, because it appeared to be too small, around 10^{-6} D, to be evaluated precisely. The four transitions mentioned here are in some way equivalent, as the final states are affected by the same Darling–Dennisson resonance between the first overtones of the two stretchings. Since from H$_2$O to D$_2$O the frequencies are all divided by the same factor (2$^{1/2}$), one expects the same vibrational interactions in both isotopomers. One could also expect similar transition moments for the cold and the hot bands, if the vibrational

interactions occurring in the region of the 012 state correspond to those acting around the 002 state.

We will try to demonstrate hereafter that an appropriate variational optimisation, like the one obtained from the VCASSCF method, can bring quantitative information on the relative importance of mode couplings and put such hypotheses into question.

3.1 Computational details

3.1.1 Potential energy and dipole moment surfaces. Both surfaces were computed by numerical derivation at the CASSCF/IC-MRCI level [8–11] using the MOLPRO [12] package. The basis set is Dunning's standard correlation consistent VQZ [13], in which the *f* function on the hydrogen as well as the *g* function on the oxygen have been eliminated, while some diffuse *s* and *p* functions were added in order to get a good value of the dipole moment (one *s* and one *p* with a 0.094 exponent on the oxygen and one *s* with a 0.054 exponent on the hydrogen).

The active set used in the CASSCF calculations includes all the core and valence electrons. The importance of the core orbitals into the active space has been demonstrated by preliminary test calculations; these show indeed that limiting the electron correlation to the valence shells only induces a deviation of $95 \, cm^{-1}$ of the antisymmetric stretch harmonic frequency. The influence of the core-valence correlation effects on the harmonic force field has been reported recently on diatomic species [14].

The MRCI configurational set was built on the complete CASSCF reference, respectively leading to 66 000 and 131 000 contracted CSFs[1], for C_{2v} and C_s geometries. We included the Davidson correction to compute the potential energy surface. The calculations were performed on a grid of 35 points defined by Rosenberg et al. [15].

The potential surface was fitted to a fourth-order SPF [16] expansion in valence coordinates and transformed to a sixth-order normal coordinate expansion using the SURVIB [17] program. The harmonic frequencies were slightly adjusted to reproduce the experimental values of the fundamental frequencies at our best level of approximation, i.e. FCI(500) (see Sect. 3.1.2). The electric dipole moment vectors, computed on each point of the grid, were rotated to the Eckart axis system, according to Le Sueur et al. [18]; they were then expanded to a third-order expansion in valence coordinates and transformed to a third-order normal coordinates expansion.

The total energy and dipole moment values, calculated at the grid points, are listed in Table 2 and the corresponding potential energy and dipole moment functions are given in Table 3. The values of the pure *ab initio* and adjusted harmonic frequencies are compared to experimental values [19, 20] in Table 4. This comparison shows that the adjustment is relatively small and leads to harmonic frequencies close to those obtained from a fit to experimental data, proving the good consistency of our model. Other calculated properties (equilibrium geometry and value of the dipole moment at this geometry) characterising the quality of the *ab initio* surfaces are compared to experimental values [21, 22] in Table 5.

---

[1] These numbers respectively correspond to 1.137 and 2.271 millions of uncontracted configurations

Table 2. Potential energy and dipole moment surfaces computed at the VQZ/IC-MRCI level

R_{OH_1} (Bohr)	R_{OH_2} (Bohr)	HOH (deg)	E^a (Hartree)	$\mu_z{}^b$ (Debye)	$\mu_x{}^b$ (Debye)
1.7509599	1.7509599	101.449	− 0.3822722	1.908036	0
1.7509599	1.7509599	104.449	− 0.3826671	1.866119	0
1.7509599	1.8109599	104.449	− 0.3835914	1.873902	− 0.024996
1.7590599	1.8409599	104.449	− 0.3832974	1.877547	− 0.036947
1.7509599	1.7509599	107.449	− 0.3826035	1.822609	0
1.7809599	1.7809599	98.449	− 0.3830894	1.956676	0
1.7809599	1.7809599	101.449	− 0.3838515	1.916054	0
1.7809599	1.8109599	101.449	− 0.3841010	1.919821	− 0.011625
1.7809599	1.7809599	104.449	− 0.3841387	1.873883	0
1.7809599	1.8109599	104.449	− 0.3843353	1.877658	− 0.017329
1.7809599	1.7809599	107.449	− 0.3839740	1.830115	0
1.7809599	1.8109599	107.449	− 0.3841213	1.833634	− 0.01306
1.7809599	1.7809599	110.449	− 0.3833822	1.784641	0
1.8109599	1.8109599	98.449	− 0.3837037	1.964308	0
1.8109599	1.8109599	101.449	− 0.3843545	1.923402	0
1.8109599	1.8109599	104.449	−·0.3845375	1.881005	0
1.8109599	1.8109599	107.449	− 0.3842755	1.836969	0
1.8109599	1.8109599	110.449	− 0.3835921	1.791224	0
1.8409599	1.8409599	98.449	− 0.3833517	1.971247	0
1.8409599	1.7809599	101.449	− 0.3838651	1.923408	0.022870
1.8409599	1.8109599	101.449	− 0.3841227	1.926828	0.011238
1.8409599	1.8409599	101.449	− 0.3838950	1.930098	0
1.8409599	1.7809599	104.449	− 0.3840469	1.881004	0.024256
1.8409599	1.8109599	104.449	− 0.3842548	1.884308	0.011933
1.8409599	1.8409599	104.449	− 0.3839777	1.887440	0
1.8409599	1.7809599	107.449	− 0.3837838	1.836991	0.025744
1.8409599	1.8109599	107.449	− 0.3839450	1.840143	0.012679
1.8409599	1.8409599	107.449	− 0.3836218	1.843136	0
1.8409599	1.8409599	110.449	− 0.3828501	1.797127	0
1.8709599	1.8709599	101.449	− 0.3825761	1.936077	0
1.8709599	1.7509599	104.449	− 0.3825696	1.881004	0.048500
1.8709599	1.7809599	104.449	− 0.3833248	1.884293	0.035792
1.8709599	1.8109599	104.449	− 0.3835384	1.887421	0.023458
1.8709599	1.8709599	104.449	− 0.3825623	1.893116	0
1.8709599	1.8709599	107.449	− 0.3821162	1.848572	0

[a] Energies given as (− 76 + E) Hartrees, Davidson correction for quadruple excitations included
[b] Rotated to the Eckart axes

3.1.2 Resolution of the vibrational problem. Different levels of approximation have been used. All of them are developed in the same framework (mainly use of the Watson Hamiltonian [6], sixth-order potential and LCHO expansion) and vary only by the degree at which mode couplings are taken into account, directly or indirectly. By *direct coupling*, we mean that some configurations implying excitations on the coupled oscillators are explicitly involved in an MCSCF or CI step. By *indirect coupling*, we mean that some mode oscillators are optimised in the mean field generated by the others, without any crossed interaction between the two sets.

Table 3. VQZ/IC-MRCI quartic force field in internal coordinates (SPF for bond stretches) and adjusted sextic force field in normal coordinates. The units are consistent with: energies in Hartrees, distances in atomic units, angles in radians and normal coordinates in atomic units

Constant[a]	Internal coordinates	Normal coordinates	Constant[a]	Normal coordinates
k_{11}	8.89421E − 01	1.52209E − 04	k_{11111}	4.92465E − 10
k_{12}	− 1.99603E − 02		k_{11112}	2.12330E − 10
k_{13}	5.73514E − 02		k_{11122}	− 1.19825E − 09
k_{22}	8.89421E − 01	2.82568E − 05	k_{11133}	5.21275E − 09
k_{23}	5.73514E − 02		k_{11222}	− 3.96129E − 10
k_{33}	8.16337E − 02	1.61206E − 04	k_{11233}	1.60191E − 09
k_{111}	− 2.06796E − 01	3.23031E − 06	k_{12222}	1.26795E − 10
k_{112}	− 2.90453E − 02	2.77819E − 07	k_{12233}	− 4.24438E − 09
k_{113}	4.59644E − 02		k_{13333}	2.72045E − 09
k_{122}	− 2.90453E − 02	− 6.88512E − 07	k_{22222}	3.27348E − 11
k_{123}	− 1.04946E − 01		k_{22233}	− 4.48577E − 10
k_{133}	− 3.61491E − 02	9.95319E − 06	k_{23333}	3.59134E − 10
k_{222}	− 2.06796E − 01	− 1.32786E − 07	k_{111111}	4.16858E − 12
k_{223}	4.59644E − 02		k_{111112}	3.45567E − 12
k_{233}	− 3.61491E − 02	9.62297E − 07	k_{111122}	− 2.17596E − 11
k_{333}	− 2.68715E − 02		k_{111133}	7.04857E − 11
k_{1111}	− 2.98508E − 01	4.50872E − 08	k_{111222}	− 1.05850E − 11
k_{1112}	− 4.72153E − 02	9.97846E − 09	k_{111233}	3.32428E − 11
k_{1113}	1.90195E − 02		k_{112222}	7.71859E − 12
k_{1122}	− 1.97480E − 02	− 4.58071E − 08	k_{112233}	− 1.53777E − 10
k_{1123}	− 1.01511E − 01		k_{113333}	7.47666E − 11
k_{1133}	− 4.80406E − 02	2.79299E − 07	k_{122222}	2.71611E − 12
k_{1222}	− 4.72153E − 02	− 1.03448E − 08	k_{122233}	− 3.22211E − 11
k_{1223}	− 1.01511E − 01		k_{123333}	2.22699E − 11
k_{1233}	7.33028E − 02	5.32921E − 08	k_{222222}	− 1.95017E − 14
k_{1333}	2.63499E − 02		k_{222233}	1.16679E − 11
k_{2222}	− 2.98508E − 01	− 7.19058E − 10	k_{223333}	− 2.66521E − 11
k_{2223}	1.90195E − 02		k_{333333}	5.19435E − 12
k_{2233}	− 4.80406E − 02	− 5.77159E − 08		
k_{2333}	2.63499E − 02			
k_{3333}	− 6.60474E − 03	4.82321E − 08		

[a] For internal coordinates, indices 1,2 and 3, respectively, refer to the SPF coordinates of both OH stretches and to the HOH angle; for normal coordinates they refer to the symmetric stretch, the bending and antisymmetric stretch normal coordintes

The VCASSCF method allows to mix both kinds of coupling: by declaring some oscillators active in a series of "active" modes and restraining the occupation on the other modes to the fundamental oscillator, one allows a direct representation of the coupling between the active modes, and an indirect representation of the coupling between active and inactive modes. Of course, the interactions between the inactive modes are also indirect.

Furthermore, the separation is very sharp; all the possible direct couplings are included in the active space, but all the other interactions are represented in an effective way, although still in a fully variational scheme. These features will be exploited as a tool for analysing stretch–bend interactions in H_2O and D_2O. The

Table 4. Harmonic frequencies of H_2O and $D_2O\,(cm^{-1})$

Frequency	Ab initio	Adjusted	Exp.[a]
ω_1	3837.8	3834.4	3832.2
ω_2	1661.1	1649.4	1648.5
ω_3	3944.4	3945.1	3942.5
D_2O			
ω_1	2766.7	2765.0	2762.8
ω_2	1215.7	1202.0	1206.4
ω_3	2889.8	2886.0	2888.8

[a] Reference [19] for H_2O; Ref. [20] for D_2O

Table 5. Equilibrium properties of the ground electronic state of water

Property	Ab initio	Exp.
R_{OH_1} (Å)	0.9568	0.9578[a]
R_{OH_2} (Å)	0.9568	0.9578[a]
HOH(deg)	104.22	104.48[a]
μ_z(D)	1.884	1.855[b]

[a] Reference [21]
[b] Reference [22]

following levels of calculation will be considered to achieve this purpose:

- complete neglect of mode coupling UAO^2
- effective representation of mode coupling   VSCF
- direct representation of stretching mode   VCASSCF(12)
  interactions and effective representation of the
  coupling with the bending mode
- direct representation of stretching mode   VCASSCF(24) to
  interactions and direct representation of the   VCASSCF(84)
  coupling with the bending mode, up to various
  energy levels
- direct, but not fully variational, representation   CI(92)
  of all modes interactions
- reference, exact variational limit of the basis set   FCI(500)

The notation VCASSCF(m) or CI(m) indicates the size m of the configuration space actually used in the variational calculation. All the CASSCF wave functions are optimised for the average of the two states implied in the transition, in order to get a pair of orthogonal wave functions, which is not the case in a VSCF optimisation. The active spaces contain in all cases the oscillators of quantum numbers 0–3 on the symmetric stretching and 0–4 on the antisymmetric stretching. They only differ by the upper limits on the bending oscillators, the lower limit being always fixed to 0. Upper limits of 0, 1, 2, 3 and 6, respectively, lead to CASSCF

---

[2] For uncoupled anharmonic oscillators, as defined in [23]

configuration sizes of 12, 24, 36, 48 and 84. In all cases the oscillators basis set has been limited to 10 harmonic oscillators per mode.

The CI(92) refers to a selection of the configurations on the following criteria: all excitations are considered up to $v = 4$ on the two stretching modes and up to $v = 6$ on the bending, every possible combination being taken as long as the sum of all vibrational quantum numbers is not greater than 10. The FCI(500) wave function corresponds to a full CI in a 10 oscillators per mode basis set; it is converged [7] with respect to both oscillators and configurations basis sets and will therefore serve here as reference level of calculation.

The notation VCASSCF(m) /CI(n) will be used below; it refers to a two-step variational procedure in which a CI(n) is performed using an oscillators basis set optimised in a previous VCASSCF(m) calculation.

3.2 Vibrational energies

The vibrational energies corresponding to all vibrational states featuring a sum of quantum numbers of 2 or less (11 states) are listed in Table 6 for the two isotopomers. These were computed using the best converged vibrational calculation (FCI(500)) in the potential surfaces described above. The adjustment on the fundamental bands gives a consistent improvement of the results for all states, with an average discrepancy with respect to experiment [24], going from 12 to 3 cm^{-1} on H_2O. This justifies the choice of evaluating the harmonic part of the potential empirically, taking account of an *ab initio* determination of the anharmonic part. This latter level of approximation should give a good description of the corresponding vibrational wave functions and will therefore be used systematically for

Table 6. Vibrational transition energies of H_2O and D_2O calculated using different potential energy surfaces

State	Ab initio	Adjusted	Exp.[a]
H_2O			
0 1 0	1607	1596	1595
0 2 0	3178	3155	3151
1 0 0	3662	3657	3657
1 1 0	5250	5233	5253
2 0 0	7218	7207	7201
0 0 2	7449	7446	7445
0 0 1	3756	3755	3756
0 1 1	5341	5328	5331
1 0 1	7265	7258	7250
D_2O			
0 1 0	1194	1179	
0 2 0	2368	2339	
1 0 0	2675	2672	2672
1 1 0	3859	3842	
2 0 0	5299	5294	5292
0 0 2	5542	5533	
0 0 1	2793	2789	2788
0 1 1	3988	3969	3956
1 0 1	5385	5377	5374

[a] Reference [24] for H_2O; Ref. [20] for D_2O

the calculation of transition moments. The set of experimental data available [20] on D_2O does not allow a complete comparison but it is clear that this heavier system is less anharmonic and is easier to represent.

3.3 Transition dipole moments

3.3.1 Analysis of transition moments. Among the transition moments calculated earlier [7] using TZ + 2P/SD-CI surfaces, the one corresponding to the 000 → 002 transition was poorly estimated to one-third of the experimental value. The reason for this comes out if one analyses the contribution of the different terms in the dipole moment expansion.

Let us write the transition dipole moment matrix element between two orthogonal state functions $|\Psi_v\rangle$ and $|\Psi_{v'}\rangle$ as

$$\bar{\mu}_{v,v'} = \sum_{i=1}^{3n-6} \frac{\partial \bar{\mu}}{\partial Q_i} \langle \Psi_v / Q_i | \Psi_{v'} \rangle + \frac{1}{2} \sum_{j=1}^{3n-6} \sum_{i=1}^{3n-6} \frac{\partial^2 \bar{\mu}}{\partial Q_i \partial Q_j} \langle \Psi_v | Q_i Q_j | \Psi_{v'} \rangle$$
$$+ \frac{1}{6} \sum_{k=1}^{3n-6} \sum_{j=1}^{3n-6} \sum_{i=1}^{3n-6} \frac{\partial^3 \bar{\mu}}{\partial Q_i \partial Q_j \partial Q_k} \langle \Psi_v | Q_i Q_j Q_k | \Psi_{v'} \rangle, \tag{10}$$

where $\bar{\mu}$ is the dipole moment surface, Q_i is the ith normal coordinate and the derivatives of $\bar{\mu}$ are calculated at the equilibrium geometry.

If we evaluate the different orders contribution, as in Table 7, we see that the sum of the second- and third-order contributions is of the same order of magnitude as the first-order term but of opposite sign. The final value will then be extremely sensitive to the value of the different contributions. In particular, mode coupling could have a great influence on the relative value of the different terms. The comparison of the different methods used to compute the dipole moments should enable us to determine the relative importance of the various possible interactions.

The efficiency of the computational method is not only measured by its ability to give a converged value of the dipole moment. As one hopes to concentrate a maximum of information on the wave function in a minimal set of configurations by variationally optimising the oscillators, a good way of measuring the compactness of the wave function is to evaluate how many configurations contribute significantly (to 1%, at least) to the total value of the dipole moment. If we express the vibrational Ψ_v wave function as a multiconfigurational expansion,

$$\Psi_v = \sum_i c_i^v \Psi_i^v, \tag{11}$$

Table 7. Relative importance of the different orders terms in the diple moment expansion for the calculation of transition moments in H_2O^a (10^{-2} D)

Transition	First-order contribution	Second-order contribution	Third-order contribution	Total value (*ab initio*)	Exp.[b]
000 → 002	− 0.1351	0.1996	− 0.00656	0.06379	0.10
010 → 012	0.1116	− 0.2183	0.01652	0.09020	

[a] Level of calculation VQZ/IC-MRCI for both potential and dipole moment surfaces and FCI (500) for the vibrational problem
[b] See Ref. [24]

where the $\{c_i^v\}$ are the CI coefficients and the $\{\Psi_i^v\}$ represent the configurations set, the transition moment (10) can be rewritten as

$$\bar{\mu}_{v,v'} = \sum_i \sum_j c_i^v c_j^{v'} \langle \Psi_i^v | \bar{\mu} | \Psi_j^{v'} \rangle. \tag{12}$$

This latter expression decomposes the transition moment to a sum of such contributions of pairs of configurations. If the two wave functions are efficiently optimised, the total dipole moment should be distributed on a relatively small number of contributions. If not, a large number of contributions will be required, making the important terms harder to spot.

3.3.2 Results and discussion. The transition dipole moments calculated at the various levels of approximation described in Sect. 3.1.2 are listed in Table 8. The number of pairs of configurations (see Eq. (12)) that contribute for at least 1% of the total value of the transition moment are also reported.

Let us first compare the UAO and VSCF values to the reference FCI(500) calculation. Although the UAO values are on average twice as large as the FCI ones, they should be regarded as much better than the VSCF ones, which are typically two orders of magnitude too large. The reason for this is the non-orthogonality of the two VSCF wave functions implied in the transition. Indeed, the large value of the permanent dipole moment in water ($\mu_e = 1.884$ D) generates an important unphysical 0th-order contribution $\langle \mu_e \langle \Psi_v | \Psi_{v'} \rangle$ to the total dipole transition moment.

Table 8. Effect of mode couplings on the computation of transition moments (10^{-2} D); the numbers in parentheses correspond to the pairs of configurations (see Eq. (12)) that contribute for at least 1% of the total value of the transition moment

Method	Transition 000 → 002		Transition 010 → 012	
H$_2$O				
UAO	4.56E − 02		3.86E − 02	
VSCF	5.26		6.47	
VSCF/CI(92)	6.08E − 02	(159)	7.69E − 0.2	(303)
VCASSCF(12)	8.80E − 02	(22)		
VCASSCF(24)	1.85E − 02	(62)	6.86E − 02	(61)
VCASSCF(36)	6.40E − 02	(65)	8.62E − 02	(74)
VCASSCF(48)	6.32E − 02	(65)	8.04E − 02	(105)
VCASSCF(84)	6.36E − 02	(65)	9.21E − 02	(109)
VCASSCF(36)/CI(92)	6.48E − 02	(95)	9.30E − 02	(192)
FCI(500)	6.38E − 02		9.03E − 02	
D$_2$O				
UAO	5.38E − 02			
VSCF	4.22			
VSCF/CI(92)	1.71E − 02	(166)		
VCASSCF(12)	1.36E − 02	(32)		
VCASSCF(24)	4.09E − 02	(43)		
VCASSCF(36)	1.40E − 02	(75)		
VCASSCF(48)	1.40E − 02	(77)		
VCASSCF(84)	1.38E − 02	(80)		
VCASSCF(36)/CI(92)	1.37E − 02	(133)		
FCI(500)	1.38E − 02			

The large discrepancies observed between the UAO and FCI(500) values clearly indicate the importance of mode couplings for such a calculation in all cases.

Let us now focus on the H_2O isotopomer and first on the 000 → 002 transition. The complete neglect of direct coupling with the bending mode (VCASSCF (12)) seems to give reasonable results, only 30% larger than the FCI reference value. However this looks fortuitous since the inclusion of the first excited bending oscillator in the active space (VCASSCF(24)) worsens this result; one has to include a further excited bending oscillator to see the dipole moment converge to the reference value. The comparison between the VCASSCF involving 36, 48, 84 configurations and the VSCF/CI(92) methods shows that the VCASSCF gives a much better result with more restricted CI expansions. This is particularly striking if one considers the number of pairs of configurations contributing significantly to the total dipole moment, the VSCF/CI calculation requires more than twice as many contributions. The comparison between the VCASSC(36) /CI(92) and VSCF/CI(92) calculations seems the fairest since the final set of configurations is the same; it still clearly shows the superiority of the VCASSCF oscillators optimisation, although the final wave function is obviously distributed on a larger number of configurations than the pure VCASSCF wave functions.

In D_2O, the same behaviour is observed for the corresponding transition, with the same oddity at the VCASSCF(24) level.

For the 010 → 012 transition the results are similar, although the VCASSCF(24) does not look like a particular case. However, the solution converges much slower to the FCI(500) value and larger CI expansions are to be used. The importance of highly excited bending oscillators appears clearly by comparing the different VCASSCF results; this is illustrated in Fig. 2, where the three
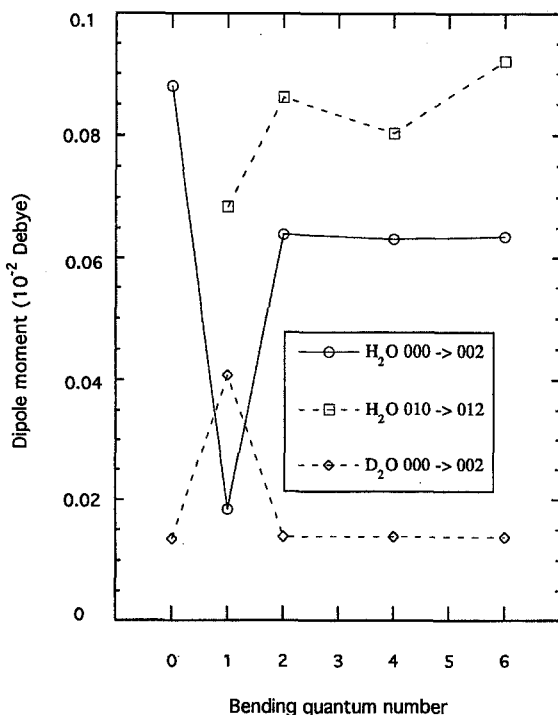

Fig. 2. Effect of excited bending oscillators on the calculated value of transition dipole moments in H_2O and D_2O

transition moments studied are plotted against the level of bending excitation taken into account. This plot clearly shows the crucial effect of stretch–bend interaction in such pure stretching transitions. The variation between the $000 \rightarrow 002$ and $010 \rightarrow 012$ transition moments is another indication that this coupling is important and felt differently in the two states.

This kind of information is crucial to people who want to interpret intensity features and understand, for instance, where does overtone intensity come from. It is moreover a basic data in the refinement of dipole moment functions starting from experimental infrared intensities; indeed, if the model used for this purpose does not include those stretch–bend coupling effects, the dipole moment surface could get seriously biased.

4 Conclusion

The extension of the VMCSCF algorithm to a VCASSCF version has proved interesting in two ways. First it makes the optimisation procedure much more efficient with the possibility of including a greater number of configurations in the MC expansion. Secondly it gives a different point of view in the interpretation of mode couplings; the discussion on the importance of particular configurations is replaced by a discussion on the effects of particular mode oscillators. The CASSCF approach provides a very neat definition of the level at which mode couplings are taken into account and allows to determine which vibrational motions are most relevant in the evaluation of a vibrational property.

This latter advantage has been illustrated in the computation of two pure stretching transitions in H_2O and D_2O. A complete methodological comparison has allowed to show the crucial importance of stretch–bend interactions for these particular transitions.

Some improvements are still to be made in order to get a real quantitative *ab initio* determination of weak transition moments. However, as it is, the procedure can be used as a guide to experimental interpretation of spectroscopic data. In particular, the efforts presently made by several research groups (see for instance [25]) to refine polyatomic potential surfaces could be completed by a refinement of *ab initio* dipole moment surfaces to give a more complete description of infrared spectra. Work along this line [26] is under progress in our group.

References

1. Culot F, Liévin J (1994) Theoret Chim Acta 89:227
2. Roos BO (1987) In: Lawley KP (ed) Advances in chemical physics, *ab initio* methods in quantum chemistry, Part 2, Vol LXVII. Wiley, New York, p 399
3. Ruedenberg K, Schmidt MW, Gilbert MM, Elbert ST (1982) Chem Phys 71:41
4. Grein F, Chang TC (1971) Chem Phys Lett 91:149
5. Bramley MC, Handy NC (1993) J Chem Phys 68:608
6. Watson JKG (1968) J Mol Spectrosc 15:479
7. Culot F, Liévin J (1992) Physica Scripta 46:502
8. Werner HJ, Knowles PJ (1985) J Chem Phys 82:5053

 9. Knowles, PJ, Werner HJ (1985) Chem Phys Lett 115:259
10. Knowles PJ, Werner HJ (1988) Chem Phys Lett 145:514
11. Werner HJ, Knowles PJ (1985) J Chem Phys 89:5803
12. MOLPRO is a package of *ab initio* programs written by Werner HJ and Knowles PJ, with contributions from Almlöf J, Amos RD, Deegan MJO, Elbert ST, Hampel C, Meyer W, Peterson K, Pitzer R, Stone AJ and Taylor PR
13. Dunning TH (1988) J Chem Phys 90:1007
14. Bauschlicher CW, Partridge H (1994) J Chem Phys 100:4329
15. Rosenberg BJ, Ermler WC, Shavitt I (1976) J Chem Phys 65:4072
16. Simons G, Parr RG, Finlan JM (1973) J Chem Phys 59:3229
17. Harding LB, Ermler WC (1985) QCPE Bull 6:25
18. Le Sueur CR, Miller S, Tennyson J, Sutcliffe BT (1992) Mol Phys 76:1147
19. Speirs GK, Spirko V (1975) J Mol Spectrosc 56:104
20. Benedict WS, Gailar N, Plyer EK (1956) J Chem Phys 24:1139
21. Hoy AR, Mills IM, Strey G (1972) Mol Phys 24:1265
22. Clough SA, Beers Y, Klein GP, Rothman LS (1973) J Chem Phys 59:2254
23. Romanovski H, Bowman JM, Harding LB (1985) J Chem Phys 82:4155
24. Rothman LS, Gamache RR, Tipping RH, Rinsland CP, Smith MAH, Benner DC, Devi VM, Flaud JM, Camy-Peyret C, Perrin A, Goldman A, Massie ST, Brown LR, Toth RA (1992) J Quant Spectrosc Radiat Transfer 48:5556
25. Bramley MJ, Carter S, Handy NC, Mills IM (1993) J Mol Spectrosc 157:301
26. Liévin J, Abbouti Temsamani M, Gaspard P, Herman M (1995) Chem Phys 190:419